Bounding the charm Yukawa coupling

Nina M. Coyle,[1] Carlos E. M. Wagner,[1,2,3] and Viska Wei[1]

[1]*Physics Department and Enrico Fermi Institute, University of Chicago, Chicago, Illinois 60637, USA*
[2]*Kavli Institute for Cosmological Physics, University of Chicago, Chicago, Illinois 60637, USA*
[3]*High Energy Physics Division, Argonne National Laboratory, Argonne, Illinois 60439, USA*

(Received 2 July 2019; published 24 October 2019)

The study of the properties of the observed Higgs boson is one of the main research activities in high-energy physics. Although the couplings of the Higgs to the weak gauge bosons and third-generation quark and leptons have been studied in detail, little is known about the Higgs couplings to first- and second-generation fermions. In this article, we study the charm quark–Higgs coupling in the so-called κ framework. We emphasize the existence of specific correlations between the Higgs couplings that can render the measured LHC Higgs production rates close to the Standard Model (SM) values in the presence of large deviations of the charm coupling from its SM value, $\kappa_c = 1$. Based on this knowledge, we update the indirect bounds on κ_c through a fit to the precision Higgs measurements at the LHC. We also examine the limits on κ_c arising from the radiative decay $H \to J/\psi + \gamma$, the charm-quark-associated Higgs production, charm-quark decays of the Higgs field, charge asymmetry in $W^{\pm} + H$ production, and differential production cross section distributions. Estimates for the future LHC sensitivity on κ_c at the high-luminosity run are provided.

DOI: 10.1103/PhysRevD.100.073013

I. INTRODUCTION

The Standard Model (SM) of particle physics provides a renormalizable and gauge-invariant description of particle interactions. It therefore makes testable predictions which are being probed at high-energy physics experiments [1]. No clear evidence of a departure of the SM-predicted behavior has been observed. However, while the predicted gauge interactions have been tested with great precision [2–5], the tests of the interactions of the recently discovered Higgs boson have not yet reached the same level of accuracy.

The Higgs production at the LHC has been probed in many different channels and the rates are in agreement with the SM-predicted ones at the level of a few tens of percent [6–8]. Since in the SM those rates are mostly governed by the coupling of the Higgs to weak gauge bosons and third-generation quarks, this suggests that the observed Higgs production rates are governed by SM interactions and that those couplings are within tens of percent of their SM-predicted values. Global fits to the Higgs precision measurements confirm this picture, showing no clear evidence of new physics coupled to the Higgs [6,8].

In spite of these facts, it is still very relevant to continue studying the properties of the Higgs boson in great detail. First of all, there could be deviations from the SM predictions at a level not yet probed by the LHC, which may reveal the presence of new physics at the weak scale. Second, the couplings to the first and second generations of quarks and leptons have not been tested and deviations from their SM-predicted values may point towards a more complex mechanism of mass generation than the one present in the SM. Third, there may be decays of the Higgs bosons into exotic particles not yet detected by the LHC. Last but not least, there may be hidden correlations between the Higgs couplings that may lead to rates in agreement with the SM-predicted ones, in spite of deviations of the couplings from the SM values. In this work, we shall present examples of such possible correlations.

In this work, we shall study possible effects of the deviations of the charm quark–Higgs coupling with respect to the SM value in the κ framework [9,10], in which κ_i characterizes the ratio of a given coupling with respect to its SM value. Large deviations of κ_c from one affect the Higgs width and therefore its decay branching ratios, and therefore the couplings of the Higgs to gauge bosons and third-generation fermions must be modified as well in order to preserve the agreement with experimental observations. We shall study these modifications in detail and discuss their impact on the determination of the charm-quark coupling to the Higgs boson.

Let us emphasize that the κ framework cannot replace a more complete study of the Higgs properties based on higher-order operators coming from integrating out the new physics at the TeV scale [11–14]. In particular, important effects related to for instance the energy dependence of the form factors associated with these operators, or the correlation of the modification of the Higgs couplings with electroweak precision measurements, are missed in the κ framework. However, this framework is appropriate to obtain an estimate of the possible sensitivity to unknown couplings, like the one of the charm quark to the Higgs, where the current bounds are far from the SM values. Moreover, the κ framework is used by the ATLAS and CMS collaborations and hence allows a direct comparison with the experimental results for values of $\kappa_c \simeq 1$.

The article is organized as follows. In Sec. II, we shall determine the specific correlations between the Higgs couplings that are necessary to keep the LHC Higgs production rates close to the SM ones. Using these results, in Sec. III we shall study the constraints that current precision Higgs measurements impose on the Higgs couplings. In Sec. IV we shall discuss the bounds on the Higgs couplings coming from the measurement of radiative decays of the Higgs boson into charmonium states. Finally, in Sec. V we shall discuss the impact of LHC Higgs production and decay rates induced by the charm coupling. We reserve Sec. VI for our conclusions.

II. BEST-FIT VALUES ON HIGGS RATES

The rate of a Higgs production and decay process relative to the Standard Model rate is represented by the signal strength μ_{if}, where

$$\mu_{if} = \frac{\sigma_i \times B_f}{(\sigma_i \times B_f)^{\mathrm{SM}}}, \tag{1}$$

is the ratio of the product of the Higgs production cross section σ_i in a given i channel and its decay branching ratio B_f in a given f channel to their SM predicted values. Within the κ framework, the quantity $\sigma_i \times B_f$ can be obtained by a simple rescaling of each coupling by a corresponding factor κ and it is therefore expressed as

$$\sigma_i \times B_f = \kappa_{r,i}^2 \sigma_i^{\mathrm{SM}} \times \frac{\kappa_f^2 \Gamma_f^{\mathrm{SM}}}{\Gamma_H} \tag{2}$$

where $\kappa_{r,i}$ is associated with the relevant Higgs coupling governing the i production mode, while κ_f is associated with the Higgs coupling governing the decay into particles f, with the SM partial width Γ_f^{SM}. The total Higgs width Γ_H is hence calculated as

$$\begin{aligned}\Gamma_H = \Gamma_H^{\mathrm{SM}} &(\kappa_b^2 B_{bb}^{\mathrm{SM}} + \kappa_W^2 B_{WW}^{\mathrm{SM}} + \kappa_g^2 B_{gg}^{\mathrm{SM}} + \kappa_\tau^2 B_{\tau\tau}^{\mathrm{SM}} + \kappa_Z^2 B_{ZZ}^{\mathrm{SM}} \\ &+ \kappa_c^2 B_{cc}^{\mathrm{SM}} + \kappa_\gamma^2 B_{\gamma\gamma}^{\mathrm{SM}} + \kappa_{Z\gamma}^2 B_{Z\gamma}^{\mathrm{SM}} + \kappa_s^2 B_{ss}^{\mathrm{SM}} + \kappa_\mu^2 B_{\mu\mu}^{\mathrm{SM}})/ \\ &(1 - B_{BSM}) \qquad (3) \\ \equiv \Gamma_H^{\mathrm{SM}} &\kappa_H^2, \qquad (4)\end{aligned}$$

where B_f^{SM} is the decay branching ratio in a given f channel within the SM and B_{BSM} is the branching ratio of the Higgs decay into beyond-the-SM particles. Here and in the following we treat the loop-induced coupling of the Higgs to gluons and photons as independent quantities, and therefore they are not restricted to the loop contributions of only SM particles.

The rates relative to the SM ones in this framework are therefore written as

$$\mu_{if} = \frac{\kappa_{r,i}^2 \kappa_f^2}{\kappa_H^2}. \tag{5}$$

It is important to remark that, considering the photon and gluon couplings as independent variables, the Higgs production rates in the standard channels (gluon fusion, weak boson fusion and associated production of the Higgs with gauge bosons, and top and bottom pairs) are not affected in any relevant way by the charm Yukawa coupling. However, the decay rates are affected in a clear way by a modification of κ_c. Indeed, the value of κ_c influences κ_H^2, therefore decreasing the rates of the observed processes by increasing the total width. Because we are interested in finding an upper bound on $|\kappa_c|$, we will not include a nonzero B_{BSM} term, which would have the same effect on the rates as increases in $|\kappa_c|$.

In order to obtain bounds on $|\kappa_c|$, we examine how well the measured rates can be fitted for increasing values of the charm Yukawa. The fit includes the most recent 13 TeV results for the observed rates from ATLAS, contained in Refs. [6] and [7], and CMS, contained in Ref. [8]. We fit to a weighted average of the experiments' measurements. The free parameters included in our fit are $\{\kappa_b, \kappa_W, \kappa_t, \kappa_Z, \kappa_\tau, \kappa_g, \kappa_\gamma\}$ with κ_c as an input. We examine three scenarios: one in which the values of κ_W and κ_Z are unconstrained, one based on estimates of the bounds coming from precision electroweak measurements, and the last in which κ_W, $\kappa_Z \leq 1$. The latter situation is less general but is well motivated by theory. We take $\kappa_{Z\gamma}$, κ_s, and κ_μ to be equal to 1 since they are not directly involved in the fitted processes and may contribute in a relevant way to the total width only for extreme values of their respective κ values.

While performing a fit to the Higgs couplings based on only the currently measured production rates, we found that no meaningful bound on κ_c could be obtained. The reason for this behavior is the existence of a flat direction in the fit for which all κ's increase along with the increasing κ_c. This fact was already emphasized for instance by the authors of Refs. [15–18], who noticed that no additional, unobserved

decays may be constrained by a simple fit to the observed production and decay rates. Although this observation was related to a possible invisible decay width, it can also be applied to the case of unobserved decays into charm quarks, in which case, by a suitable modification of the κ_i, the observed rates can be modeled equally well for any value of κ_c. To see this, we can write down the rate for a given observed process as

$$\mu_{if} = \frac{\kappa^4}{\kappa^2(1 - B_{cc}^{\rm SM}) + \kappa_c^2 B_{cc}^{\rm SM}} \tag{6}$$

where since all $\mu_{if} \simeq 1$ we have considered that all non-charm Higgs couplings scale together by a single κ value. If we require the signal strengths μ_{if} to be given by a value μ, Eq. (6) provides a quadratic equation in κ^2. The solution to this quadratic equation leads to a correlation between the necessary values of the generic κ and κ_c, namely

$$\kappa^2 = \frac{(1 - B_{cc}^{\rm SM})\mu}{2} + \frac{\sqrt{(1 - B_{cc}^{\rm SM})^2\mu^2 + 4\mu B_{cc}^{\rm SM}\kappa_c^2}}{2}. \tag{7}$$

Since, as stressed before, the observed rates are all within tens of percent of the SM values, one should require $\mu \approx 1$ in order to obtain agreement with the precision Higgs measurements. Therefore, given that $B_{cc}^{\rm SM} \simeq 0.03$, an unconstrained fit to all couplings will lead to the following approximate correlation between the Higgs couplings:

$$\kappa^2 \approx \frac{0.97}{2} + \frac{\sqrt{(0.97)^2 + 0.12\kappa_c^2}}{2} \tag{8}$$

which clearly has a solution for all real κ_c.

III. CONSTRAINTS ON κ_c FROM HIGGS PRECISION MEASUREMENTS

The existence of the flat direction described in Eq. (8) implies that no constraints on the κ_c values may be obtained by considering only the current Higgs precision measurements. Additional constraints are therefore necessary to put a bound on κ_c. In this section, we shall describe the constraints imposed by the bounds on the total Higgs width, the ones coming from precision electroweak measurements, and finally the ones coming from the theoretical prejudice that, in most extensions of the SM, $\kappa_V \leq 1$.

In all cases we perform a fit to κ_c marginalizing over all the other couplings. The channels included in the fit are shown in Table I. In addition to the individual decay channels listed in the table, we also include the combined results for each given production mode. We combine the ATLAS and CMS results given in Refs. [6–8] by a weighted average, weighting by the squared inverse of the respective 1σ uncertainties. The uncertainty in the combined observation is given by

TABLE I. The production and decay channels included in the fit over κ's. We also include the combined results for each production mode.

Production mode	Decay mode	Production mode	Decay mode
ggF	$H \to \gamma\gamma$	VH	$H \to \gamma\gamma$
	$H \to ZZ$		$H \to ZZ$
	$H \to WW$		$H \to bb$
	$H \to \tau\tau$		
VBF	$H \to \gamma\gamma$	ttH	$H \to \gamma\gamma$
	$H \to ZZ$		$H \to VV$
	$H \to WW$		$H \to \tau\tau$
	$H \to \tau\tau$		$H \to bb$

$$\sigma_{if}^{\rm comb.} = \frac{1}{\sqrt{1/(\sigma_{if}^{\rm ATLAS})^2 + 1/(\sigma_{if}^{\rm CMS})^2}} \tag{9}$$

where σ_{if} indicates the uncertainty in the corresponding observed value of μ_{if}.

The χ^2 value for a given fit is calculated as

$$\chi^2 = \sum_{if} \frac{(\mu_{if}(\kappa) - \mu_{if}^{\rm obs})^2}{\sigma_{if}^2} \tag{10}$$

where $\mu_{if}(\kappa)$ represents the calculated value of μ_{if}, using Eq. (5), for the given set of κ's. We find the best fit at each κ_c by minimizing the value of χ^2 for the given κ_c.

In the cases where κ_V is constrained, we obtain a 95% C.L. bound by placing a limit on $\Delta\chi^2$ relative to the best fit at $\kappa_c = 1$. In order to identify the appropriate $\Delta\chi^2$ cut, we performed a principle component analysis [19,20] on a centralized data set of $\{\kappa_b, \kappa_W, \kappa_t, \kappa_\tau, \kappa_Z, \kappa_\gamma, \kappa_g\}$ for $\kappa_c \in [1.0, 4.0]$, for $\kappa_V \leq 1$. We converted the seven-dimensional correlated κ data into a set of uncorrelated principle components, and observed that the 99%-dominant principle component is an approximately equally weighted linear combination of $\{\kappa_b, \kappa_t, \kappa_\tau, \kappa_\gamma, \kappa_g\}$. κ_W and κ_Z contribute trivially to the principle direction due to the constraint $\kappa_V \leq 1$. Thus we treat $\{\kappa_b, \kappa_W, \kappa_t, \kappa_\tau, \kappa_Z, \kappa_\gamma, \kappa_g\}$ as one fit parameter. Including the fit parameter coming from κ_c, our χ^2 fit is effectively a two-parameter fit. As a result, we will employ a 95% C.L. cut corresponding to $\Delta\chi^2 = 5.99$.

A. Higgs decay width

The increase in all κ's following the flat direction described in Eq. (8) leads to an increase in the total width Γ_H, and one may therefore place a bound on $|\kappa_c|$ using bounds on the Higgs width. ATLAS and CMS have performed maximum likelihood fits using on-shell and off-shell $H \to ZZ$ measurements to obtain a bound on the total Higgs width; they found

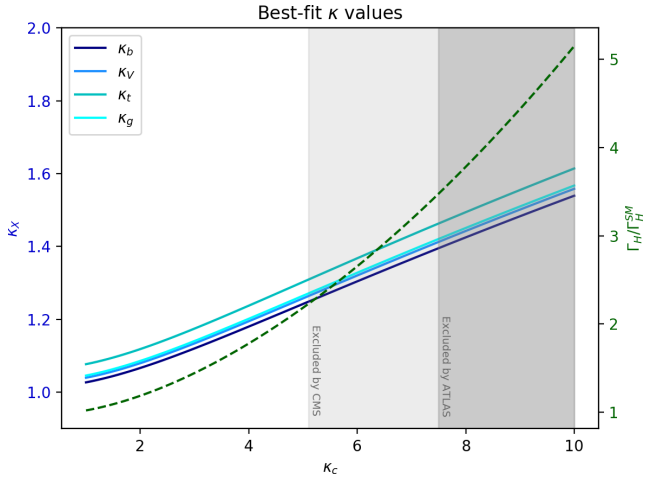

FIG. 1. Plots of the best-fit values of κ's, represented by solid lines, to the precision rate measurements μ_{if}. The grey regions are excluded by constraints on the total Higgs width, which is normalized to the SM value and represented by a dashed line.

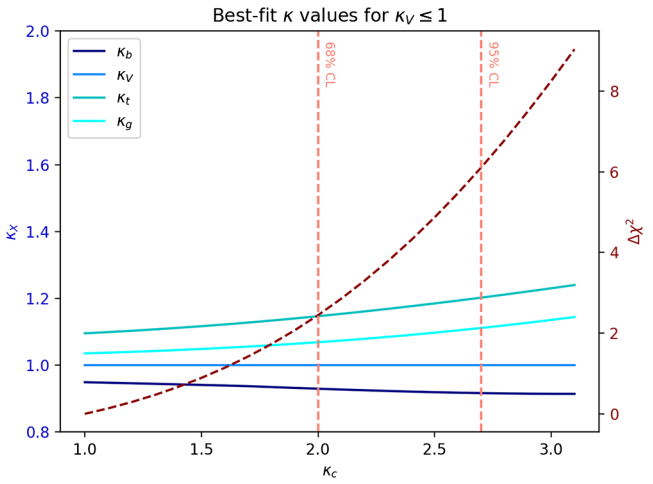

FIG. 2. Plots of the best-fit values of κ's for $\kappa_V \leq 1$. Although we plot κ_W and κ_Z together as κ_V, the two differ very slightly due to the differences in the W and Z rate measurements. The dashed line represents the $\Delta\chi^2$ of the fit at a given κ_c relative to the χ^2 of the fit at $\kappa_c = 1$.

$$\Gamma_H < 14.4 \text{ MeV} \quad \text{(ATLAS)},$$
$$\Gamma_H < 9.16 \text{ MeV} \quad \text{(CMS)}, \tag{11}$$

or $\Gamma_H/\Gamma_H^{\text{SM}} < 3.5$ and $\Gamma_H/\Gamma_H^{\text{SM}} < 2.2$, respectively, at 95% C.L. [21,22]. It is necessary to note that these limits are obtained by making certain assumptions, in particular that the κ values do not depend on the momentum transfer of the Higgs production mechanism and that $\kappa_V = \kappa_g$. Because κ_V and κ_g naturally have nearly equal values in the best fits, this second condition is indeed approximately satisfied.

We perform a χ^2 fit to the LHC measurements of all measured signal strengths μ_{if}, Eq. (5), for increasing values of κ_c and find that the 95% C.L. limits on the Higgs width lead to a bound of $|\kappa_c| < 7.5$ from ATLAS and $|\kappa_c| < 5.1$ from CMS. Figure 1 shows a plot of the best-fit κ's for increasing κ_c, and indicates the regions for which the total Higgs width, represented by the dashed line, exceeds the current bounds. The spread in values for the various κ's arises from the differences in individual rate measurements.

B. Precision electroweak measurements

It is also worth noting that the necessary increases in all κ values to be consistent with the Higgs production rates result in $\kappa_V > 1$. In particular, for $|\kappa_c| = 7.5$ the least-squares fit gives values of $\kappa_W = 1.42$ and $\kappa_Z = 1.38$, which are consistent with the approximate flat direction values given by Eq. (8). These large values for κ_V result in divergences in electroweak precision parameters which are not canceled by the Higgs contribution, as they are in the SM. In this case one would require an extension of the SM which cancels the divergent contributions to the precision measurement variables. One can replace the divergence by a parametric logarithmic dependence on an effective cutoff that characterizes the new physics. In such a case, for instance, if one assumes a cutoff scale of the order of $\Lambda = 3$ TeV, a fit to the precision electroweak measurements leads to a value of $\kappa_V = 1.08 \pm 0.07$ [23]. Since κ_V is now constrained to values lower than the ones necessary to reach the bounds on the Higgs width, there will be a stronger upper bound on κ_c.

In order to find a bound on κ_c from this limit on κ_V, we include the deviation of κ_V from $\kappa_V = 1.08$ in the calculation of χ^2 and perform a χ^2 fit for increasing κ_c. We examine the $\Delta\chi^2$ relative to the fit at $\kappa_c = 1$. Performing a fit to the Higgs rates using this constraint on κ_V, one obtains $|\kappa_c| < 4.9$. Observe, however, that this bound depends on specific assumptions about the new physics scale.

C. Constrained κ_V

In this third scenario, the flat direction is removed by constraining $\kappa_W, \kappa_Z \leq 1$. This constraint is well motivated, as models with extended Higgs sectors such as a two-Higgs-doublet model will typically include couplings to the weak gauge bosons lower than the SM values for the individual Higgs particles. Similarly to the previous case, the κ's cannot increase uniformly to maintain the same relative strengths, so we expect that the fit will become less accurate as the total width increases through κ_c. As in the previous section, we obtain a 95% C.L. bound on κ_c by identifying the value of κ_c for which the least-squares fit has $\Delta\chi^2 = 5.99$ relative to the best fit at $\kappa_c = 1$. We find a bound of $|\kappa_c| < 2.7$ at 95% C.L. Figure 2 shows a plot of the behavior of the best-fit κ's, represented by solid lines, for increasing κ_c along with the value of $\Delta\chi^2$, represented by a dashed line.

D. Future prospects for the HL-LHC

We can examine these cases for the HL-LHC, for which the projected uncertainties of the rate measurements have been examined for ATLAS [24] and CMS [25]. We update the 1σ uncertainties used in our χ^2 fit using the combined expected errors quoted in the two studies. In the case of the width constraint, if only the on-shell rate measurements are considered, the bound on $|\kappa_c|$ remains approximately the same, as the κ values along the flat direction are similar regardless of the uncertainties in μ_{if}. However, the width bound is also expected to improve with higher luminosity. According to an ATLAS study of off-shell Higgs to ZZ measurements for the HL-LHC [26], assuming the observed on-shell and off-shell rates are equal to the SM prediction, the expected determination of Γ_H with 3 ab^{-1} is

$$\Gamma_H = 4.2^{+1.5}_{-2.1}\ \text{MeV} \tag{12}$$

or $\Gamma_H/\Gamma_H^{\text{SM}} = 1.0^{+0.4}_{-0.5}$. Requiring that the width remains consistent with this expectation corresponds to a bound of $|\kappa_c| \lesssim 3.0$.

The projected constraints for $\kappa_V \leq 1$ depend somewhat on the values of μ_{if} one uses in the fit. The projection studies use $\mu_{if} = 1$ for all initial and final states to estimate the percent uncertainty on each measurement. An alternative method is to adjust the percent uncertainty to the expected HL-LHC values but use the current measurements; this method is not ideal, as limiting the uncertainties without changing the values of μ_{if} is unlikely to accurately reflect the HL-LHC results. However, the comparison of the bounds on κ_c obtained in the two scenarios provides a good picture of the likely constraints on this quantity. For μ_{if} equal to the current measurements, we find an expected bound of $|\kappa_c| < 2.2$. On the other hand, for $\mu_{if} = 1$, the expected bound is given by $|\kappa_c| < 2.1$. We therefore expect the HL-LHC to provide an indirect limit of $|\kappa_c| \lesssim 2.1$ in the $\kappa_V \leq 1$ case.

IV. RADIATIVE HIGGS DECAY TO J/ψ

Radiative decays of the Higgs boson into charmonium states are known to provide a sensitive probe of the charm coupling, and have been previously examined in this context in Refs. [27–30]. This is due to the fact that the charm-coupling-induced rates interfere with those induced by the top and W couplings in a well-defined way. For instance, the width for $H \to J/\psi + \gamma$ is given by [31]

$$\Gamma(H \to J/\psi + \gamma) = |(11.9 \pm 0.2)\kappa_\gamma - (1.04 \pm 0.14)\kappa_c|^2 \times 10^{-10}\ \text{GeV} \tag{13}$$

where the first term arises from the amplitude which contains no dependence on κ_c and the second from the κ_c-dependent amplitude. Plugging in $\kappa_\gamma, \kappa_c = 1$ and $\Gamma_H^{\text{SM}} = 4.195 \times 10^{-3}$ GeV gives the SM value for the branching ratio as

$$BR^{\text{SM}}(H \to J/\psi + \gamma) = 2.79 \times 10^{-6}. \tag{14}$$

The current bound on this process is

$$\sigma \times \text{BR}(H \to J/\psi + \gamma) < 19\ \text{fb} \tag{15}$$

at 95% C.L. Assuming the SM production cross section [32], this limit corresponds to

$$\text{BR}(H \to J/\psi + \gamma) < 3.5 \times 10^{-4}. \tag{16}$$

Since the production cross section depends on the values of the κ's, which should increase together with $|\kappa_c|$ in order to maintain agreement with the Higgs production rates, this bound on the branching ratio is only useful for moderate values of κ_c, for which $\sigma_H \approx \sigma_H^{\text{SM}}$. However, the bound on the branching ratio is 2 orders of magnitude larger than the SM branching ratio, and therefore cannot currently probe moderate values of κ_c. Additionally, the branching ratio displays asymptotic behavior for large κ_c, as there are also κ_c-dependent enhancements of the Higgs total width. For large κ_c, the approximate expression for the branching ratio along the flat direction is given by

$$\text{BR}(H \to J/\psi + \gamma) \approx \frac{(5|\kappa_c|^{1/2} - 1.04\kappa_c)^2 \times 10^{-10}\ \text{GeV}}{(0.16|\kappa_c| + 0.03\kappa_c^2) \times \Gamma_H^{\text{SM}}}. \tag{17}$$

Figure 3 shows a plot of the behavior of this Higgs radiative decay branching ratio along the flat direction as

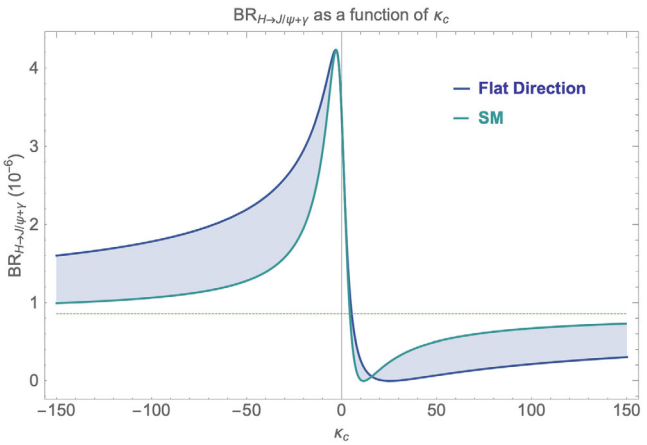

FIG. 3. Plot of the branching ratio of $H \to J/\psi + \gamma$ varying along the flat direction (dark blue) and with other Higgs couplings fixed to SM values (light blue). The expected asymptote of approximately 8×10^{-7} is indicated by the green dashed line.

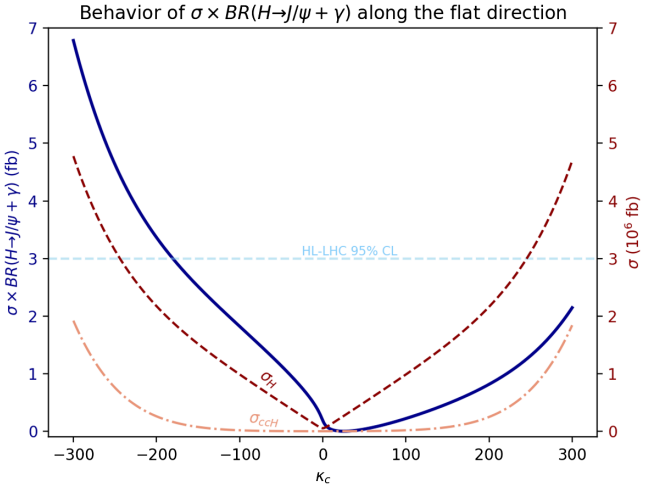

FIG. 4. Plot of $\sigma \times \mathrm{BR}(H \to J/\psi + \gamma)$ for the flat direction. The blue line indicates $\sigma \times BR$ in fb, while the pink dot-dashed (dashed) lines indicate the $c\bar{c}H$ (total) production cross section in fb. The dashed grey line shows the expected HL-LHC 95% C.L. bounds.

well as with SM-like values for the other couplings. We stress again that setting the other Higgs couplings to SM values for large $|\kappa_c|$ does not align well with rate measurements from the LHC, and it is therefore more instructive to examine the flat direction for large $|\kappa_c|$. In both cases, the branching ratio peaks at moderate negative values of κ_c, at a maximum value of approximately 4×10^{-6}, 2 orders of magnitude below the current limit for SM production rates.

Given the non-SM production rate and asymptotic behavior of the branching ratio for large κ_c, we consider the limit on $\sigma \times BR$ rather than only the branching ratio. The production cross section increases due to both κ^2 enhancements given by Eq. (8) as well as κ_c-dependent processes such as $c\bar{c}H$ production, which become relevant for very large κ_c. We fit data produced with MadGraph5 [33] at leading order (LO) to obtain an expression for the approximate scaling of $\sigma_{c\bar{c}H}$ for large κ_c at 13 TeV, which is given by

$$\sigma_{c\bar{c}H} \approx |5.24 \times 10^{-2} + 2.76 \times 10^{-2}\kappa_c - 5.45 \times 10^{-6}\kappa_c^2 + 1.30 \times 10^{-6}\kappa_c^3|^2 \text{ pb}. \quad (18)$$

We also include contributions to VH production from $c + \bar{c}/\bar{s}$ initial states. Figure 4 shows a plot of $\sigma \times BR_{J/\psi}$ in fb for the flat direction.

Considering properly the rate, instead of just the radiative decay branching ratio, a limit can now be set for very large values of κ_c. By the end of the HL-LHC, the expected 95% C.L. upper bound on $\sigma \times \mathrm{BR}(H \to J/\psi + \gamma)$ from ATLAS will be approximately 3 fb [34]. We therefore expect this process to place a limit of $\kappa_c \in [-180, 330]$ at the HL-LHC for the flat direction. This limit is 2 orders of magnitude larger than those from other HL-LHC prospects discussed previously. A strong improvement, of an order of magnitude of the present expected sensitivity, would be necessary for this channel to provide a competitive bound on κ_c.

The authors of Ref. [31] have updated the partial width expression with a new approach to the resummation of logarithms, and quote a new width of [35]

$$\Gamma(H \to J/\psi + \gamma) = |(11.71 \pm 0.16)\kappa_V - ((0.627^{+0.092}_{-0.094}) + i(0.118^{+0.054}_{-0.054}))\kappa_c|^2. \quad (19)$$

This expression has a reduced dependence on κ_c, and therefore gives even weaker bounds on κ_c than those found above.

It is important to note that such large values of κ_c encounter strong experimental and theoretical issues. On the one hand, following the flat direction in order to retain consistency with precision Higgs measurements leads to large values of the top-quark coupling to the Higgs $g_{ht\bar{t}}$. In particular, for values of $\kappa_c \gtrsim 100$ one requires values of $\kappa_t \gtrsim 17$. In this case, the value of $g^2_{ht\bar{t}}$ is greater than 4π, and a perturbative examination of the Higgs sector becomes unreliable. One may attempt to avoid this issue by fixing κ_t to be less than a certain value, in which case the Higgs rates would become inconsistent with those observed at the LHC. We therefore note that such large values of κ_c are problematic for either LHC Higgs rates or perturbativity concerns. Moreover, as stressed in Sec. III, unless a very particular momentum dependence of the effective couplings is present, large values of $\kappa_c \gg 10$ would lead to a value of the Higgs width that is in strong tension with current LHC measurements.

V. HIGGS PRODUCTION RATES INDUCED BY THE CHARM-HIGGS COUPLING

As stressed before, Higgs production may be induced in proton collisions via its coupling to the charm quark. Moreover, the Higgs boson may decay into charm quarks and may be detected in this decay channel, provided these decays may be disentangled from the ones into bottom quarks.

A. Higgs associated production with charm quarks

The cH production mode has also been proposed as a search method for κ_c. Because this channel has a lesser dependence on κ_c at very large $|\kappa_c|$ than $c\bar{c}H$, it was not included in the analysis of radiative Higgs decays in Sec. IV. However, the cH channel has a higher production cross section at small or moderate values of $|\kappa_c|$, preferred by the total Higgs width constraints and precision electroweak measurements analyzed in Sec. III. A previous study of this channel [36] shows that a high-luminosity LHC, with 3000 fb^{-1} integrated luminosity at ATLAS and CMS,

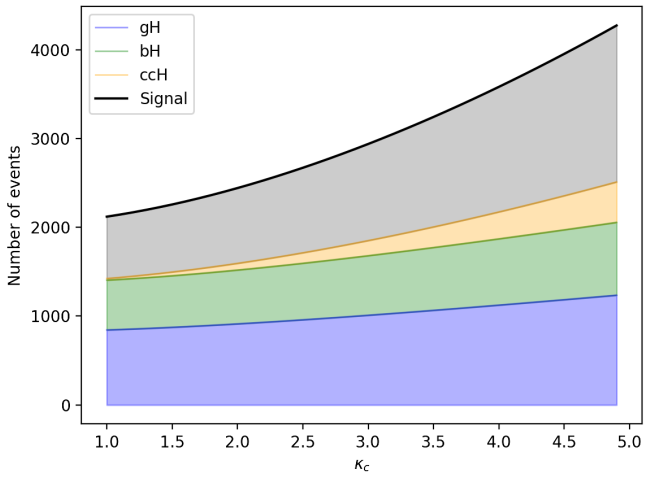

FIG. 5. The expected number of background and signal events for cH production at the HL-LHC with 3 ab^{-1} integrated luminosity.

should be able to probe values of $\kappa_c < 2.5$ at 95% C.L. This study leaves all other κ's fixed to the SM expectation, varying only κ_c, and therefore we should reanalyze it taking into account the rise of the κ_i along the flat direction.

The cH production process involves three diagrams at leading order: s-channel and t-channel diagrams with a c propagator and a $c\bar{c}H$ vertex, and an s-channel diagram with a gluon propagator and a ggH vertex. Since the diagram with the ggH vertex is dominant for SM values of the Higgs couplings, we expect that following the flat direction would further enhance the cH production beyond the values found in Ref. [36]. However, this also further enhances the background processes $pp \to gH$ and $pp \to bH$ in addition to the $pp \to c\bar{c}H$ background.

We use MadGraph at leading order in a specialized model file, which includes an effective ggH vertex, to calculate the production rates. We vary the values of κ_c and increase κ_g and κ_b proportionally according to Eq. (8) to obtain the production cross section for each process. Using a charm-tagging efficiency of 30%, a $c\bar{c}H$ mistag rate as cH of 5%, and b and g mistag rates of 20% and 1%, respectively [37], we obtain the expected number of events for $\sigma(pp \to XH) \times \mathrm{BR}(H \to \gamma\gamma)$ for 3 ab^{-1} integrated luminosity. Although $\sigma(pp \to gH) \gg \sigma(pp \to bH)$, the larger b mistag rate leads to similar background contributions from the two processes. The $c\bar{c}H$ background has a stronger dependence on κ_c and therefore contributes an increasing fraction of the background for larger κ_c. The results are shown in Fig. 5.

The cH process includes dependence on both the κ_c enhancement and the κ_g enhancement along the flat direction. It therefore increases more quickly with κ_c than the background processes, which each depend on only one of these enhancements; in particular, the dominant backgrounds of $pp \to bH, gH$ depend only on the flat direction enhancements of κ_b, κ_g. We show the number of signal and background events, along with their ratio, for a range of κ_c values in Table II.

TABLE II. The number of signal events, number of background events, and signal-to-background ratio for values of κ_c between 1 and 5. Due to the increase in κ_g, κ_b along the flat direction, the background increases in addition to the signal.

κ_c	1.0	1.5	2.0	2.5	3.0	3.5	4.0	4.5	5.0
S	687	758	840	961	1085	1230	1408	1598	1822
B	1425	1498	1595	1714	1852	2005	2174	2356	2551
S/B	0.33	0.34	0.35	0.36	0.37	0.38	0.39	0.40	0.42

Since variations in σ_{cH} depend weakly on κ_c alone along the flat direction, it would be very difficult to identify the precise value of κ_c from a measurement of $N = S + B$. However, we may use these signal and background rates to estimate the sensitivity to κ_c following a similar analysis to the one in Ref. [36]. Assuming the true value of κ_c is 1, we find the expected 1σ and 2σ upper bounds on κ_c from this process by identifying the value of κ_c for which $N(\kappa_c) - N(1) = 1\sigma, 2\sigma$. We take the statistical uncertainty to be $\Delta N^{\mathrm{stat}}(\kappa_c) = \sqrt{S(\kappa_c) + B(\kappa_c)}$ and the theoretical uncertainty in the signal and background, which we have calculated at LO, to be 20%. Because our background is now also being estimated for varying κ_c using MadGraph5, we examine two cases for the uncertainty in the background. In the first case, we apply no uncertainty to the number of background events. In the second case, we apply a 20% uncertainty to the number of background events $B(\kappa_c)$ in addition to the number of signal events. We find ΔN^{tot} by adding the statistical and theoretical uncertainties in quadrature. Let us stress that this analysis assumes that the dominant uncertainties are the statistical and theoretical ones and ignores the possible impact of systematic and experimental uncertainties. The sensitivity on κ_c depends strongly on these assumptions, and may become weaker after a realistic experimental analysis of this process is performed.

We take $\Delta N^{\mathrm{tot}} = \sigma$ to parametrize the number of standard deviations of $N(\kappa_c) - N(1) = n\sigma$ for the two uncertainty cases. The value of n is plotted versus κ_c in Fig. 6. We find 1σ (2σ) deviations for

$$|\kappa_c| < 1.6(2.1) \tag{20}$$

in the first case, and

$$|\kappa_c| < 2.5(4.0) \tag{21}$$

in the second case. In the first case the increase of the expected sensitivity relative to Ref. [36], in which no uncertainty was applied to the background estimates, arises from the enhancement of the background events in addition to the signal events. In the second case, we find approximately the same expected sensitivity as in Ref. [36].

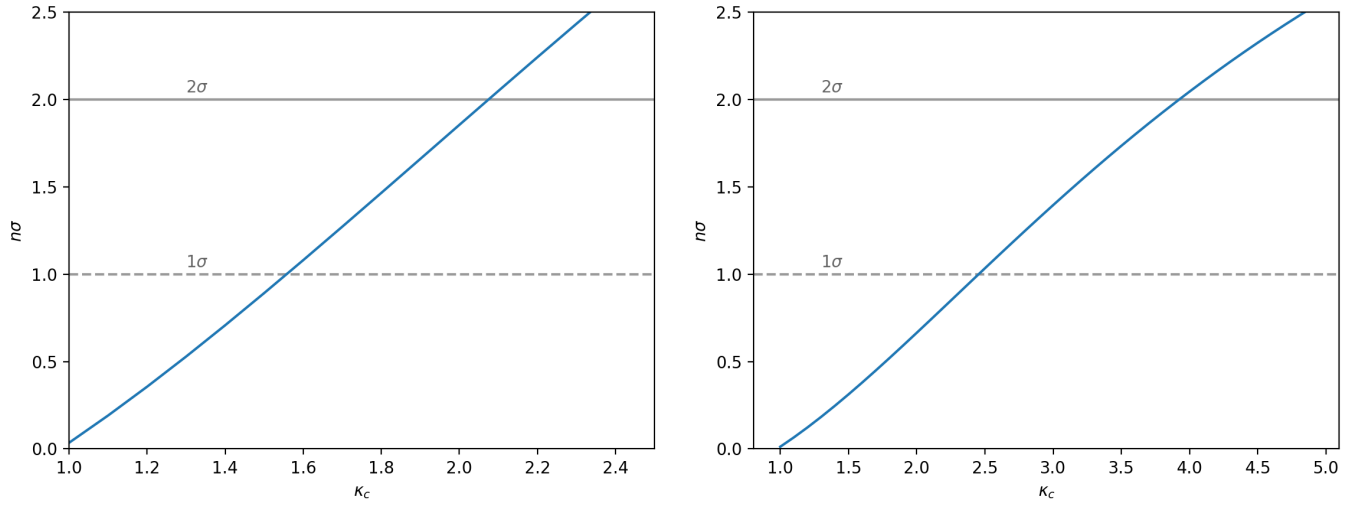

FIG. 6. Number of standard deviations of $N(\kappa_c)$ from $N(1)$, as a function of κ_c. The dashed (solid) grey lines indicate the 1σ (2σ) bounds. The two cases represent (left) no uncertainty in background and (right) 20% uncertainty on the number of background events.

Although the best-fit κ values for low values of κ_c tend to follow the flat direction, we note that taking SM-like values for the other couplings can still retain some level of consistency with LHC results for this range of κ_c; therefore, our results do not invalidate the analysis of Ref. [36] but show the variation of the LHC sensitivity for slightly larger values of κ_g, for which an improvement of the fit to the Higgs precision measurement data is obtained.

B. Higgs decay into charm-quark pairs

1. Direct searches

Searches have been performed for $ZH \to l^+l^-c\bar{c}$ with 36.1 fb^{-1} integrated luminosity, with ATLAS publishing an upper bound of $\sigma(pp \to ZH) \times B(H \to cc) < 2.7$ pb at 95% C.L. [37]. This corresponds to about 110 times the SM rate. Thus we require that $\kappa_Z^2\kappa_c^2/\kappa_H^2 \lesssim 110$; moving along the flat direction, one reaches this limit at a value of $|\kappa_c| = 20.9$, which is a far weaker bound than the one provided by the total width constraints. However, HL-LHC studies from ATLAS [38] have found an expected upper bound of $\mu_{ZH\to c\bar{c}} < 6.3$ at 95% C.L. with an integrated luminosity of 3 ab^{-1}. Unconstrained fits of the rate measurements remain within this limit for $|\kappa_c| \lesssim 2.7$; this channel may therefore provide a bound of similar magnitude to those from constrained-fit bounds at the HL-LHC.

The $ZH \to l^+l^-c\bar{c}$ limit obtained in the ATLAS HL-LHC study uses a tighter charm-tagging working point than the working point employed in Run 2, thereby reducing the background contribution from processes such as $ZH \to Zb\bar{b}$. In particular, the tagging efficiency for c jets, and mistagging rates for b jets, and light-flavor jets are 18%, 5%, and 0.5%, respectively, for the HL-LHC study, while these values are 41%, 25%, and 5% for the Run 2 analysis. This stricter working point takes advantage of the higher expected signal yield at the HL-LHC to provide a 7% additional improvement on the limit relative to Run 2. However, charm-tagging algorithms are currently being improved, in part through the use of deep neural networks. For example, CMS deep tagging algorithms have achieved a 24% tagging efficiency with 1% b-jet and 0.2% light-jet mistagging rates [39]. This algorithm therefore has a 6% improvement in efficiency over the HL-LHC study working point along with a factor of 5 improvement in the b-jet mistag rate. The use of new tagging algorithms could therefore further improve the limit obtained at the HL-LHC.

2. Indirect searches

The $H \to c\bar{c}$ decay can also be examined in the context of $H \to b\bar{b}$ decays to place a bound on κ_c using current data [27,28]. We examine the effect of $c\bar{c}$ mistagging as $b\bar{b}$ on the observed $H \to b\bar{b}$ rates. This results in κ_c being a factor in the numerator of $\mu_{i,b\bar{b}}$, thereby limiting the flat direction described by Eq. (8) for large values of κ_c. We include the $c\bar{c}$ contributions to $b\bar{b}$ rates by

$$\mu_{i,b\bar{b}} = \kappa_i^2 \frac{\kappa_b^2 + \kappa_c^2(BR_{c\bar{c}}\epsilon_c^2/BR_{b\bar{b}}\epsilon_b^2)}{\kappa_H^2} \tag{22}$$

where ϵ_c is the mistag rate of c jets as b jets and ϵ_b is the tagging efficiency of b jets and we have defined $\mu_{i,b\bar{b}}$ as the observed rate normalized to the uncontaminated SM rate. Our analysis of this bound differs from that by Perez *et al.* [28], in two primary ways. First, we include this altered expression for $\mu_{i,b\bar{b}}$ in our fit to all of the LHC observed rates listed in Table I, thereby removing the "flat direction" for $\mu_{i,b\bar{b}}$ along $\kappa_b = \kappa_c$ encountered in Ref. [27], which examined only $H \to b\bar{b}$ processes. We therefore do not need to

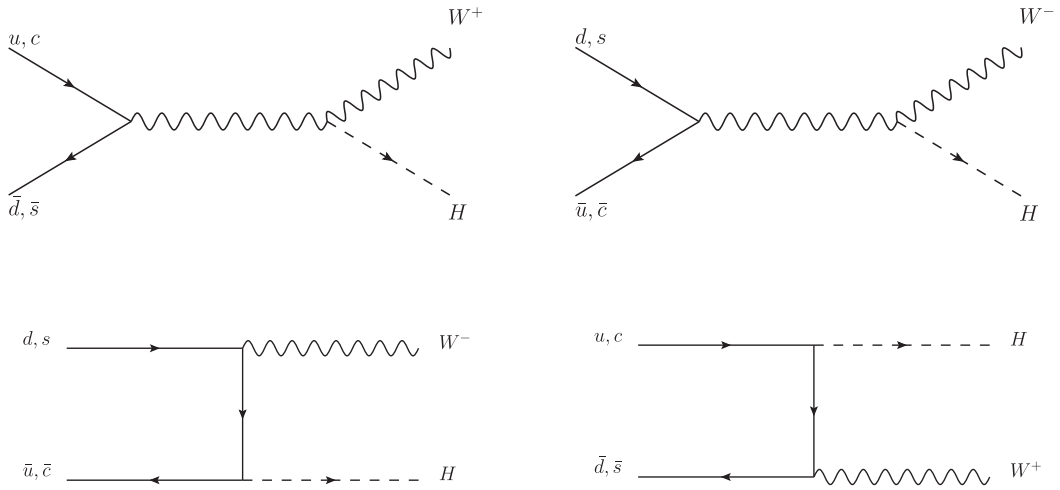

FIG. 7. Diagrams for the two relevant types of $W^{\pm}H$ production processes at leading order. The top row shows the Higgsstrahlung processes, which are dominant in the SM, while the bottom row shows the diagrams proportional to the charm Yukawa.

employ multiple tagging points to obtain a bound for κ_c, since for sizable values of κ_c, raising κ_b and κ_c together will spoil the fit to other observables. Consequently, we allow variations in the other κ's, which approximately follow the flat direction described by Eq. (8). Because of this, κ_b and κ_c may have greater variations than those found in Refs. [27,28] while remaining consistent with observed $b\bar{b}$ (and all other) Higgs rates. We therefore expect to find weaker bounds in our analysis of this potential bound.

We employ the ATLAS working point of $\epsilon_b = 0.70$, $\epsilon_c = 0.20$ and the CMS working point of $\epsilon_b = 0.78$, $\epsilon_c = 0.27$. To obtain a bound, we perform a fit to the Higgs rate measurements and place a limit on $\Delta\chi^2$. Following this analysis, the ATLAS and CMS tagging efficiencies provide bounds of $|\kappa_c| \lesssim 23$ and $|\kappa_c| \lesssim 16$, respectively. Using the HL-LHC expected uncertainties [24,25] along with best-fit rates of $\mu = 1.0$, this approach places bounds of $|\kappa_c| \lesssim 8.7$ and $|\kappa_c| \lesssim 6.5$, respectively.

C. Asymmetry in W^+H and W^-H production

The measurement of asymmetry in $\sigma(pp \to W^+H)$ and $\sigma(pp \to W^-H)$ production has also been proposed as a channel through which one can place limits on κ_c [40]. The relevant diagrams for this process are shown in Fig. 7. The SM asymmetry is driven by the Higgsstrahlung processes; in the Higgsstrahlung diagrams, the difference in W^+ and W^- production arises from the asymmetry of $u\bar{d}$ and $\bar{u}d$ in the proton parton distribution function (PDF). The charm Yukawa appears in diagrams with $s\bar{c}$ and $\bar{s}c$ initial states, which are symmetric in the proton PDF. Therefore, when the charm Yukawa is increased significantly, the symmetric $s\bar{c}/\bar{s}c$ diagrams reduce the asymmetry with respect to the SM expected value. The $W^{\pm}H$ production asymmetry therefore decreases with large κ_c. One can therefore use the sensitivity of this asymmetry on κ_c to get bounds on the charm coupling [40].

Given the relative contributions of the two types of diagrams, however, we note that enhancements of κ_W alongside enhancements of κ_c will reduce the symmetrizing effect of increasing κ_c. In order to examine this quantitatively, we use MadGraph5 to calculate the LO cross sections at 14 TeV for W^+H and W^-H production along the flat direction. Figure 8 shows the results of this analysis. We plot the percent asymmetry of the production modes, quantified as

$$A_{W^{\pm}} = \frac{\sigma_{W^+H} - \sigma_{W^-H}}{\sigma_{W^+H} + \sigma_{W^-H}}, \tag{23}$$

as a function of κ_c along the flat direction, as well as for $\kappa_X = 1$ with $X \neq c$.

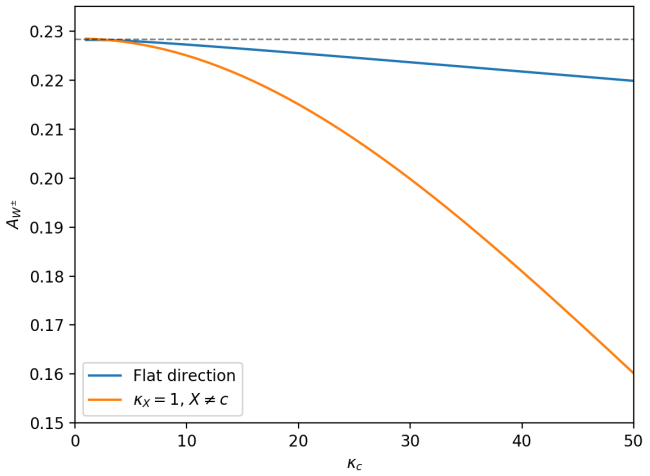

FIG. 8. Plot of the percent asymmetry in $W^{\pm}H$ production versus κ_c, for the flat direction and for SM-like κ_X, $X \neq c$. While large κ_c significantly reduces the asymmetry in the second case, the enhancement of κ_W alongside κ_c in the flat direction reduces the relative effect of the symmetrizing κ_c-proportional contributions.

We find that the asymmetry is reduced to less than 0.02 up to $\kappa_c = 100$. Using MadGraph5 and detector simulations, Ref. [40] found that the uncertainty in the asymmetry may be reduced to approximately 0.004 with 3 ab^{-1} integrated luminosity. In this case, the $W^{\pm}$ asymmetry would be able to place a limit of $|\kappa_c| \lesssim 30$ along the flat direction. This still provides a weaker bound than other proposed methods by approximately an order of magnitude, and we therefore conclude that if one requires consistency with LHC precision Higgs measurements, the $W^{\pm}H$ asymmetry does not provide a sensitive probe of κ_c.

D. Differential cross sections

The distribution of the Higgs production differential cross section as a function of transverse momentum has also been proposed as a probe of κ_c [41–43] and has been examined for 35.9 fb^{-1} of data by CMS [44]. This method of bounding κ_c may provide an interesting complementary bound to those from the fit to precision rate measurements, as the flat direction along which the rates remain constant may not reproduce the expected SM cross section distribution as a function of transverse momentum. The CMS study examines the $H \to \gamma\gamma$ and $H \to ZZ$ decay channels, as well as their combination, and identifies bounds by varying κ_b and κ_c and examining two cases: the first in which the branching fractions are dependent on $\kappa_{b,c}$, and the second in which they are independent. In the dependent case, they quote a bound of $-4.9 < \kappa_c < 4.8$, while in the independent case the bound is $-33 < \kappa_c < 38$. The uncertainties in the cross section distribution, which are on the order of 10–20%, are currently dominated by statistical uncertainty, while the systematic uncertainty is on the order of about 5%. The bounds quoted above would therefore be expected to improve with more data.

However, we again note that varying $\kappa_{b,c}$ to values as large as 5 would significantly affect the other observed channels, and that therefore the flat direction is necessary to ensure consistency with the current Higgs observations. It is likely that varying the other couplings along the flat direction will affect the bound in this case. In particular, the variation of κ_t in addition to κ_b and κ_c should affect the expected distribution and would likely weaken the identified bounds, while the branching fractions would vary less dramatically with increases in $\kappa_{b,c}$. One might expect that along the flat direction the bounds will be similar to the one found in the unconstrained case. A study of this bound with the addition of the flat direction is necessary to provide a bound on κ_c that is consistent with the other LHC measurements.

Reference [41] has predicted the possible HL-LHC bounds from the differential cross section distributions. Assuming a theory uncertainty of 2.5% and systematic uncertainty of 1.5%, they found a 95% C.L. bound of $\kappa_c \in [-0.6, 3.0]$. However, we emphasize that these bounds do not take into account the rate measurements and the flat direction, and also assume significant improvements in the theoretical and systematic uncertainties.

VI. CONCLUSIONS

After the Higgs discovery, one of the main goals of the high-energy program is the detailed study of its properties. In particular, the measurement of the Higgs couplings to SM bosons and fermions is of crucial importance. Most of the Higgs production and decay processes measured at the LHC are sensitive to the gauge bosons and third-generation quark and lepton Yukawa couplings and therefore, considering only variations of these couplings, they are being determined within an accuracy of the order of tens of percent.

The first- and second-generation quark and lepton couplings are, however, not yet determined. In particular, the Yukawa coupling of the charm quark, characterized by κ_c in the κ framework, is only weakly constrained. In this work we updated the bounds on κ_c, paying particular attention to the consistency with the LHC Higgs precision measurements. In this sense, we discussed the existence of particular correlations between the charm coupling and the gauge boson and third-generation couplings that allow consistency with the measured Higgs process rates, even for large deviations of κ_c.

Due to the existence of these correlations, a bound on κ_c may only be obtained by imposing additional constraints. These are provided by bounds on the Higgs width, precision measurements, and $|\kappa_V| \leq 1$, leading to a 95% C.L. bound on $|\kappa_c| < 7.5$, 4.9, and 2.7, respectively. The Higgs width and $|\kappa_V| \leq 1$ bounds may be improved at higher luminosities to values of order $|\kappa_c| \lesssim 3.0$ and 2.1, respectively.

We also analyzed radiative decays of the Higgs into quarkonium states, explaining the relevance of the flat direction and the variations of the Higgs width and the production rate. No competitive bound on κ_c from LHC data may be obtained, even at high luminosities.

Finally, we studied Higgs processes induced by the charm-quark Yukawa coupling. These include both Higgs production in association with charm quarks as well as possible decays of the Higgs into charm states. While currently all these searches cannot provide a competitive bound on κ_c, the possible improvements in charm tagging at higher luminosities may lead to a sensitivity that is similar to the one obtained from precision Higgs measurements, namely $|\kappa_c| \lesssim 2$ and 2.7 in the cH and $ZH, H \to c\bar{c}$ channels, respectively. The effect of κ_c on the differential Higgs production cross section may also provide a competitive bound, but it will demand an improvement in the current theoretical and systematic uncertainties. Moreover, a careful examination of this bound, taking into account all observed Higgs rates, should be performed.

ACKNOWLEDGMENTS

We thank Javier Duarte, Florian Goertz, Gino Isidori and Konstantinos Nikolopoulos for useful discussions. Work at A. N. L. is supported in part by the U.S. Department of Energy under Contract No. DE-AC02-06CH11357. The work of C. W. and N. C. at E. F. I. is supported by the U.S. Department of Energy under Contract No. DE-FG02-13ER41958. V. W. is supported by the University of Chicago Physics Department.

[1] M. Tanabashi *et al.* (Particle Data Group), Phys. Rev. D **98**, 030001 (2018).
[2] Tevatron Electroweak Working Group (CDF and D0 Collaborations), arXiv:1204.0042.
[3] S. Schael *et al.* (ALEPH, DELPHI, L3, OPAL, SLD Collaborations and LEP Electroweak Working Group, SLD Electroweak Group, SLD Heavy Flavour Group), Phys. Rep. **427**, 257 (2006).
[4] T. S. Electroweak (LEP, ALEPH, DELPHI, L3, OPAL Collaborations and LEP Electroweak Working Group, SLD Electroweak Group, SLD Heavy Flavor Group), arXiv:hep-ex/0312023.
[5] S. Schael *et al.* (ALEPH, DELPHI, L3, OPAL, and LEP Electroweak Collaborations), Phys. Rep. **532**, 119 (2013).
[6] ATLAS Collaboration, CERN Report No. ATLAS-CONF-2018-031, 2018.
[7] M. Aaboud *et al.* (ATLAS Collaboration), Phys. Lett. B **786**, 59 (2018).
[8] A. M. Sirunyan *et al.* (CMS Collaboration), Eur. Phys. J. C **79**, 421 (2019).
[9] A. David *et al.* (LHC Higgs Cross Section Working Group), arXiv:1209.0040.
[10] S. Heinemeyer *et al.* (LHC Higgs Cross Section Working Group), CERN Report no. CERN-2013-004, 2013, https://dx.doi.org/10.5170/CERN-2013-004.
[11] R. S. Gupta, A. Pomarol, and F. Riva, Phys. Rev. D **91**, 035001 (2015).
[12] R. Contino, M. Ghezzi, C. Grojean, M. Muhlleitner, and M. Spira, J. High Energy Phys. 07 (2013) 035.
[13] A. Falkowski, Pramana **87**, 39 (2016).
[14] D. de Florian *et al.* (LHC Higgs Cross Section Working Group), *Handbook of LHC Higgs Cross Sections: 4. Deciphering the Nature of the Higgs Sector*, CERN Yellow Reports: Monographs Vol. 2 (CERN, Geneva, 2017).
[15] D. Zeppenfeld, R. Kinnunen, A. Nikitenko, and E. Richter-Was, Phys. Rev. D **62**, 013009 (2000).
[16] A. Djouadi *et al.*, arXiv:hep-ph/0002258.
[17] M. Duhrssen, S. Heinemeyer, H. Logan, D. Rainwater, G. Weiglein, and D. Zeppenfeld, Phys. Rev. D **70**, 113009 (2004).
[18] G. Belanger, B. Dumont, U. Ellwanger, J. F. Gunion, and S. Kraml, Phys. Rev. D **88**, 075008 (2013).
[19] F. R. S. Karl Pearson, London Edinburgh Dublin Philos. Mag. J. Sci. **2**, 559 (1901).
[20] H. Hotelling, J. Educ. Psychol. **24**, 417 (1933).
[21] M. Aaboud *et al.* (ATLAS Collaboration), Phys. Lett. B **786**, 223 (2018).
[22] A. M. Sirunyan *et al.* (CMS Collaboration), Phys. Rev. D **99**, 112003 (2019).
[23] A. Falkowski, F. Riva, and A. Urbano, J. High Energy Phys. 11 (2013) 111.
[24] ATLAS Collaboration, CERN Report No. ATL-PHYS-PUB-2018-054, 2018
[25] CMS Collaboration, CERN Report No. CMS-PAS-FTR-18-011, 2018.
[26] ATLAS Collaboration, CERN Report No. ATL-PHYS-PUB-2015-024, 2015.
[27] G. Perez, Y. Soreq, E. Stamou, and K. Tobioka, Phys. Rev. D **92**, 033016 (2015).
[28] G. Perez, Y. Soreq, E. Stamou, and K. Tobioka, Phys. Rev. D **93**, 013001 (2016).
[29] M. König and M. Neubert, J. High Energy Phys. 08 (2015) 012.
[30] G. T. Bodwin, F. Petriello, S. Stoynev, and M. Velasco, Phys. Rev. D **88**, 053003 (2013).
[31] G. T. Bodwin, H. S. Chung, J. H. Ee, J. Lee, and F. Petriello, Phys. Rev. D **90**, 113010 (2014).
[32] M. Aaboud *et al.* (ATLAS Collaboration), Phys. Lett. B **786**, 134 (2018).
[33] J. Alwall, R. Frederix, S. Frixione, V. Hirschi, F. Maltoni, O. Mattelaer, H.-S. Shao, T. Stelzer, P. Torrielli, and M. Zaro, J. High Energy Phys. 07 (2014) 079.
[34] M. Aaboud *et al.* (ATLAS Collaboration), CERN Technical Report. ATL-PHYS-PUB-2015-043, 2015.
[35] G. T. Bodwin, H. S. Chung, J. H. Ee, and J. Lee, Phys. Rev. D **95**, 054018 (2017).
[36] I. Brivio, F. Goertz, and G. Isidori, Phys. Rev. Lett. **115**, 211801 (2015).
[37] M. Aaboud *et al.* (ATLAS Collaboration), Phys. Rev. Lett. **120**, 211802 (2018).
[38] ATLAS Collaboration, CERN Report No. ATL-PHYS-PUB-2018-016, 2018.
[39] CMS Collaboration, CERN Report No. CMS-DP-2018-046, 2018.
[40] F. Yu, J. High Energy Phys. 02 (2017) 083.
[41] F. Bishara, U. Haisch, P. F. Monni, and E. Re, Phys. Rev. Lett. **118**, 121801 (2017).
[42] Y. Soreq, H. X. Zhu, and J. Zupan, J. High Energy Phys. 12 (2016) 045.
[43] G. Bonner and H. E. Logan, arXiv:1608.04376.
[44] A. M. Sirunyan *et al.* (CMS Collaboration), Phys. Lett. B **792**, 369 (2019).